Appl Phys B (2012) 106:683–690
DOI 10.1007/s00340-011-4775-x

Applied Physics B
Lasers and Optics

Intra-cavity generation of superpositions of Laguerre–Gaussian beams

D. Naidoo · K. Aït-Ameur · M. Brunel · A. Forbes

Received: 30 May 2011 / Revised version: 15 August 2011 / Published online: 11 October 2011

Abstract In this paper we demonstrate experimentally the intra-cavity generation of a coherent superposition of Laguerre–Gaussian modes of zero radial order but opposite azimuthal order. The superposition is created with a simple intra-cavity stop that creates equal losses for the two azimuthal modes, and we show that by adjustment of the stop we can produce modes up to azimuthal order 8. The fact that we have a coherent superposition rather than an incoherent superposition is verified by intensity measurements, propagation measurements and a decomposition of the field by an inner product executed on a phase-only spatial light modulator. Such fields have relevance in quantum information and optical trapping.

D. Naidoo · A. Forbes (✉)
Council for Scientific and Industrial Research, National Laser Centre, P.O. Box 395, Pretoria 0001, South Africa
e-mail: aforbes1@csir.co.za
Fax: +27-12-8413152

D. Naidoo · A. Forbes
School of Physics, University of KwaZulu-Natal, Private Bag X54001, Durban 4000, South Africa

K. Aït-Ameur
Centre de recherche sur les Ions, les Matériaux et la Photonique, Unité Mixte de Recherche 6252, Commissariat à l'Energie Atomique, Centre National de la Recherche Scientifique, Ecole Nationale Supérieure d'Ingénieurs de Caen, Université de Caen, 6, bd Maréchal Juin, 14050 Caen Cedex 4, France

M. Brunel
Complexe de Recherche Interprofessionnel en Aérothermochimie, Unité Mixte de Recherche 6614, Centre National de la Recherche Scientifique, Université de Rouen, Avenue de l'université BP 12, 76801 Saint Etienne du Rouvray Cedex, France

1 Introduction

It is well known that one can improve the efficacy and power extraction of a laser beam from the cavity by employing intra-cavity laser beam shaping techniques. For example, the fundamental mode of the cavity may be tailored to any desired shape by appropriate insertion of phase-only elements, to create flat-top beams [1], Gaussian beams [2] or in fact any field defined at the output coupler plane [3, 4]. Alternatively the selection of the desired mode can be enhanced by shaping the pump light [5], insertion of an appropriate obstruction [6] or by the insertion of a phase-diffractive optic [7]. However, these techniques invariably define a single mode as the output. Indeed, we have recently outlined [8] a method for the generation of a single high-order Laguerre–Gaussian mode with zero radial p order but with a non-zero azimuthal order l: LG_{0l}. It is worth considering whether it is possible to create coherent superpositions of such modes inside the laser cavity. This is interesting since such modes (single and superpositions thereof) are known to have direct relevance to studies involving the orbital angular momentum (OAM) component of light [9], for example, in optical trapping [10] and quantum information with higher-dimensional state spaces [11, 12].

LG_{0l} modes have been reported to have been experimentally generated in optically pumped [13] and electrically pumped [14] vertical-cavity surface-emitting semiconductor lasers (VCSELs). Chen et al. [6, 15] explored pumping a microchip laser with a hollow beam profile allowing for superpositions of LG_{0l} modes to oscillate. These profiles have also been reported to be experimentally generated by use of photorefractive oscillators [16], nonlinear interferometers [17], saturation of nonlinear media [18] and suppressing low order transverse mode oscillation by defecting the rear mirror with a spot in a flat–flat cavity [19]. It has to be noted that the studies are contradictory on what the observed petal-like patterns actually are: in some it is *assumed* [15] that they are single mode Laguerre–Gaussian beams, while studies external to the cavity routinely refer to such modes as superpositions. Here we *propose* that the petal patterns observed are in fact superpositions of Laguerre–Gaussian beams, but to date neither hypothesis has been tested by considering in detail the modal decomposition of the "petal" structures produced from certain cavities. In other words, it remains an hypothesis that the petal-like patterns generated in such lasers are indeed due to an equally weighted coherent superposition of two LG_{0l} modes of opposite handedness ($+l$ and $-l$).

In this paper we outline a simple experimental approach to generate petal-like transverse modes inside the laser cavity that involves only a stop to be placed on one mirror. We show that this set-up results in petal-like modes, and we propose that these petal-like profiles are the result of a coherent superposition of two equally weighted Laguerre–Gaussian modes of zero radial order but opposite azimuthal order. We perform a variety of experimental tests to verify that this hypothesis is correct, including, intensity comparisons, propagation analysis and a full modal decomposition using a phase-only spatial light modulator. The result is the first demonstration of a coherent superposition of such modes directly from a standard Fabry–Pérot laser cavity, and in a controllable (azimuthal mode number can be adjusted) manner.

2 Laguerre–Gaussian modes

We are interested in the addition of two Laguerre–Gaussian, LG_{pl}, modes, where p is the radial order and l is the azimuthal order, for which the electric field may be written as [20]

$$u_{p,l} = \sqrt{\frac{2p!}{\pi(p+|l|)!}}\frac{1}{w(z)}\left(\frac{\sqrt{2}r}{w(z)}\right)^{|l|} L_p^{|l|}\left(\frac{2r^2}{w(z)^2}\right) \times \exp\left(\frac{-r^2}{w(z)^2} - \frac{ikr^2}{2R(z)}\right) \times \exp\left[-i\left(2p+|l|+1\right)\arctan\left(\frac{z}{z_R}\right)\right]\exp(-il\phi), \tag{1}$$

where r and ϕ are the radial and azimuthal coordinates, respectively, and $L_p^{|l|}$ is the generalized Laguerre polynomial. Here the Gaussian parameters have their usual meaning, with z the propagation distance, z_R the Rayleigh range, and $R(z)$ and $w(z)$ are the radius of curvature and beam width of a Gaussian beam, respectively. From this we may note that a coherent addition of two Laguerre–Gaussian modes, both of zero radial order but having an opposite azimuthal order, may then be expressed as

$$\begin{aligned} u_{0,\pm l} &= u_{0,+l} + u_{0,-l} \\ &= \sqrt{\frac{2}{\pi(|l|)!}}\frac{1}{w(z)}\left(\frac{\sqrt{2}r}{w(z)}\right)^{|l|}\exp\left(\frac{-r^2}{w(z)^2} - \frac{ikr^2}{2R(z)}\right) \\ &\quad \times \exp\left[-i\left(|l|+1\right)\arctan\left(\frac{z}{z_R}\right)\right] \\ &\quad \times \left[\exp(il\phi) + \exp(-il\phi)\right]. \end{aligned} \tag{2}$$

We note that the expression of the sum of opposite azimuthal phases allows (2) to be expressed as

$$u_{0,\pm l} = A(r,z) \times \cos(l\phi), \tag{3a}$$

with

$$A(r,z) = 2\sqrt{\frac{2}{\pi(|l|)!}}\frac{1}{w(z)}\left[\frac{\sqrt{2}r}{w(z)}\right]^{|l|}\exp\left[\frac{-r^2}{w(z)^2} - \frac{ikr^2}{2R(z)}\right] \times \exp\left[-i\left(|l|+1\right)\arctan\left(\frac{z}{z_R}\right)\right], \tag{3b}$$

where for brevity and to aid clarity we have collapsed all the other terms into the general function $A(r,z)$. The intensity profile of this structure ($I \propto |A|^2\cos^2(l\phi)$) has $2l$ nodes in the azimuth, resulting in a pattern of "petals" around a circle. This differs substantially from what might be expected from an incoherent superposition of the modes:

$$I_{0,\pm l} \propto \left|A(r,z)\right|^2. \tag{4}$$

The fields described above in (3) and (4) also differ in their propagation characteristics. The propagation of the coherent field may be expressed as

$$u_2 = iN\exp(-ikL)\int_0^{2\pi}\int_0^{\infty} u_{0,\pm l} \times \exp\left\{-i\pi N\left[r^2 + \rho^2 - 2r^2\rho^2\cos(\theta-\phi)\right]\right\} r\,dr\,d\phi, \tag{5}$$

where N is the Fresnel number, L is the optical path length between some initial plane and an observation plane, $u_{0,\pm l}$ is the initial electric field at $z = 0$, r and ρ are the radial coordinates at the initial position and at position L, respectively, and ϕ and θ are the azimuthal coordinates at initial position and at position L, respectively. The propagation of any real (coherent) laser beam is known [21, 22] to follow a simple rule for the change in beam size with propagation distance if the beam size is defined as the second moment of the intensity [23]

$$\sigma_x^2(z) = \frac{\iint (x-\bar{x})^2 I(x,y,z)\,dx\,dy}{\iint I(x,y,z)\,dx\,dy}, \tag{6a}$$

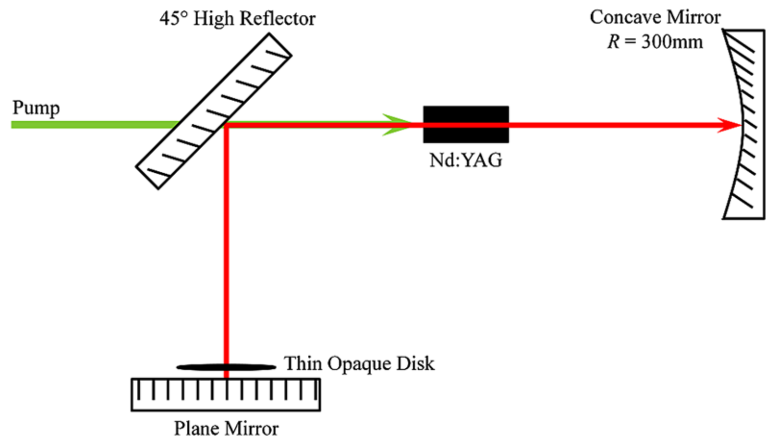

Fig. 1 Experimental se-tup where an Nd:YAG solid-state medium is longitudinally pumped with a 75 W multi-mode fiber-coupled diode. A thin opaque disk (stop) is positioned on the plane mirror and chosen to be large enough to completely obstruct Gaussian oscillation and permit higher-order mode selection

$$\sigma_x^2(z) = \sigma_{x0}^2 + \lambda^2 \sigma_{s_x}^2 (z - z_{x0})^2, \tag{6b}$$

$$W_x(z) = 2\sigma_x(z), \tag{6c}$$

where $\bar{x}$ is the first order intensity moment that is zero for azimuthally symmetric beams, $\sigma_x^2(z)$ obeys the free-space propagation rule of (6b) where $\sigma_{s_x}^2$ is the second moment of the spatial frequency distribution and $W_x(z)$ is the beam diameter. Equations (6a)–(6c) may be equally expressed in the transverse y component and in cylindrical coordinates, (6b) and (6c) are expressed as

$$\sigma_r^2(z) = \sigma_x^2(z) + \sigma_y^2(z), \tag{7a}$$

$$W_r(z) = \sqrt{2}\sigma_r(z) \tag{7b}$$

from which the laser beam quality factor can be deduced as

$$M^2 = 2\pi\sigma_r\sqrt{\sigma_{s_x}^2 + \sigma_{s_y}^2}. \tag{8}$$

It is also instructive to decompose the field, $u_{0,\pm l}$ as well as some unknown field into a series of angular harmonics, $\exp(il\phi)$. Since such harmonics are orthogonal over the azimuthal plane, we may express any field in terms of such harmonics as

$$u(r,\phi,z) = \frac{1}{\sqrt{2\pi}} \sum_l a_l(r,z)\exp(il\phi), \tag{9}$$

with

$$a_l(r,z) = \frac{1}{\sqrt{2\pi}} \int_0^{2\pi} u(r,\phi,z)\exp(-il\phi)\,d\phi. \tag{10}$$

The relative weighting of the power contained in each azimuthal mode can then be defined as

$$P_l(z) = \frac{\int_0^\infty |a_l(r,z)|^2 r\,dr}{\sum_l \int_0^\infty |a_l(r,z)|^2 r\,dr}. \tag{11}$$

From the definition of (10), one can easily show that the weighting of each harmonic for the case of a superposition of LG_{0l} modes is given by

$$a_l(r,z) = a_{-l}(r,z) = \sqrt{2\pi}A(r,z), \tag{12}$$

with all other coefficients zero.

3 Experimental set-up

There are a variety of experimental approaches used to obtain petal-like transverse modes as indicated in Sect. 1. Here we consider a plano-concave solid-state laser resonator which is end-pumped with a multi-mode fiber coupled diode. A requirement in obtaining LG_{0l} modes is to force near circular symmetry within the resonator cavity. This was achieved by inserting a thin opaque circular metal disk a very short distance away from the plane mirror; the disk was set large enough to completely obstruct the Gaussian beam oscillation. This permitted the selection of circular symmetric modes, and at high input pump powers the higher-order LG_{0l} modes were thus able to oscillate preferentially. We suppose that since the individual LG_{0l} modes in the superposition have identical losses, one is not able to differentiate between them (on a loss basis) within the laser cavity. A schematic of the experimental set-up is presented in Fig. 1.

The g parameter, which is a measure of the resonator stability is required to obey the relation $0 < g_1 g_2 < 1$ (where $g_i = 1 - L/R_i$ where $i = 1, 2$ which corresponds to the resonator mirrors, L is the length of the resonator and R is the curvature of the mirrors) was chosen to be 0.1 for a concave output coupler of 300 mm curvature. The gain medium used was a 4 mm diameter Nd:YAG rod (length of 30 mm), which was end-pumped with a Jenoptik (JOLD-75-CPXF-2P W) 75 W multi-mode fiber-coupled diode. The cavity was constructed in an L-shape to avoid obstruction of the pump beam by the thin opaque disk. The opaque disk, 200 µm in diameter, was fabricated by photolithography on a glass plate for minimal round trip losses to the unobstructed

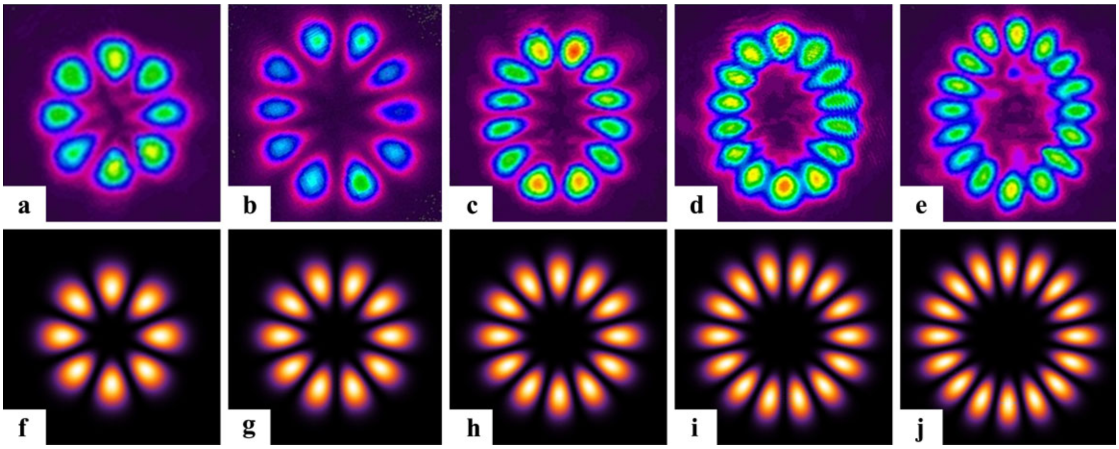

Fig. 2 A comparison between experimentally generated superpositions of LG_{0l} transverse modes, (**a**)–(**e**), and theoretically simulated profiles (**f**)–(**j**) where the azimuthal order, l, in (**a**) is 4 and increases in unit value for the subsequent experimental images

field. The Gaussian beam width on the plane mirror in the cold cavity was calculated to be ∼175 μm, or marginally (∼12%) smaller than the opaque disk.

A standard beam profiling technique was used to determine the beam quality factor of the superposition field. Upon focusing the beam through a lens, a CCD device (Spiricon LBA-USB L130) was used to scan the beam profile along the propagation axis to determine the beam width (as a second moment of the intensity) as a function of distance, from which beam waist position, beam waist width and the beam quality factor could be determined following (8).

The resulting superposition field was directed to a spatial light modulator (SLM) (Holoeye HEO 1080P) for executing the modal decomposition of (10). This was accomplished by executing an inner product of the incoming field with the pattern on the SLM (match filter) set to $\exp(il\varphi)$, for l values ranging from -10 to $+10$. Measurement of the signal at the origin of the Fourier plane (at the focal plane of a lens after the SLM) returned the intensity of the coefficients of the modal expansion.

4 Results and discussion

The measured intensity profiles of the petal-like output modes at the plane of the output coupler are illustrated in Figs. 2(a)–(e). The increase in the number of petals in the images is a direct result of an increase in the input pump power and slight realignment of the disk. These images are compared to theoretically simulated intensity profiles based on a coherent superposition of LG_{0l} modes, shown in Figs. 2(f)–(j), and clearly there are strong similarities. One notices that the experimental images tend to an oval shape with an increase in the azimuthal order: this is due to the slight misalignment of the disk as a technique to create controlled superpositions (ideally multiple disks of slightly differing sizes should be used, but unfortunately were not available to us). The very small misalignment of the disk (of typically tens of micrometers) resulting in the oval patterns is a minor perturbing factor, but appears not to be significant enough to distinguish between the handedness of the modes (as will be shown later by comparison of theory and experiment). However, this perturbation probably also accounts for the slight smearing of the petals, as can be observed in Fig. 2(d). The results shown here are typical experimental images, and clearly show a petal-like structure as the output of the laser. One can anticipate that with custom fabricated stops for each azimuthal order, results similar to those of Fig. 2(a) would be obtained. Prior to executing the full modal decomposition, which is a definitive test of the modal structure of the field, we performed a series of tests based on intensity and propagation of the field.

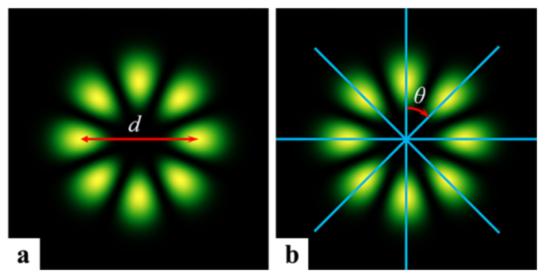

Fig. 3 An illustration of the two visually based comparisons, (**a**) peak-to-peak petal diameter, d and (**b**) angle between adjacent petals, θ, which are performed on theoretically simulated intensity profiles and experimental data

Due to the similarity of the images in Fig. 2, it was worth undertaking visually based tests as part of the verification that petal-like structures are generated from a coherent superposition of LG_{0l} modes. Two intensity-based tests were performed on the data: (i) diameter of the petal structure, and (ii) angle between adjacent petals, as illustrated in Fig. 3,

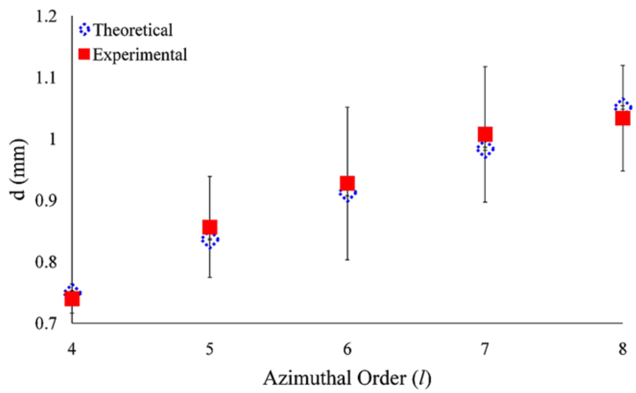

Fig. 4 A comparison of a test performed in determining the peak-to-peak petal diameter of opposing petals between theoretical and experimental data. The respective data have a high degree of correlation

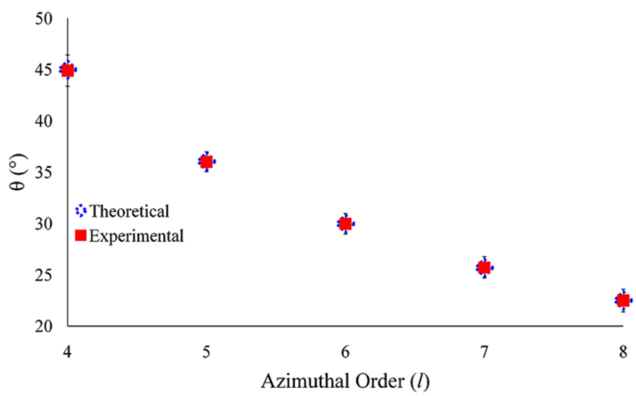

Fig. 5 A comparison is drawn between theoretical and experimental data in the determination of the angle between adjacent petals in the superposition of two LG_{0l} modes, showing good agreement

with the use of an image tool (ImageJ) to find the peak values of each petal for the calculation where the average diameter was taken to account for the oval shaped field. The experimental data were compared to those expected theoretically based on the assumption of a coherent mix of LG_{0l} modes, and the results are represented in Figs. 4 and 5 for the petal-structure diameter (d) and angle (θ) between adjacent petals, respectively.

The excellent agreement is indicative that these intensity profiles are due to a coherent superposition of LG_{0l} modes, but single plane measurements of the intensity are not sufficient to falsify the hypothesis. A study on vector beams in the generation of Laguerre–Gaussian and Bessel–Gaussian vector beams by Ito et al. [19] illustrates very similar intensity patterns as that seen in Fig. 2. These beams were generated in a slightly misaligned spot defected cavity upon passing through a linear polarizer. Upon rotating the polarizer on an incident LG_{0l} mode of l equal to 1, the petal-like intensity patterns are seen and are used to deduce that the LG_{01} mode is azimuthally polarized, however for higher orders of l, the LG_{0l} modes were deemed radially polarized. Petal-like intensity patterns are also seen for larger input powers and are understood as higher-order Bessel–Gaussian vector beams, however, no further analysis other than polarization measurements confirms this theory. In our study, the petal-like modes were vertically polarized, which can be attributed to the design of the 45° high reflector mirror that reflects (preferentially) σ-polarization, corresponding to vertically polarized light at the output. This leads us to analyze the propagation and modal decomposition to infer a superposition of two LG_{0l} modes. The experimental fields were propagated (see Fig. 6) through a lens, and the beam widths, near-field and far-field intensities measured. Following the approach outlined in the previous section, the laser beam quality factor was inferred from the measured data and compared to the theoretical value. The results, shown in Fig. 7, show excellent agreement between theory and experiment.

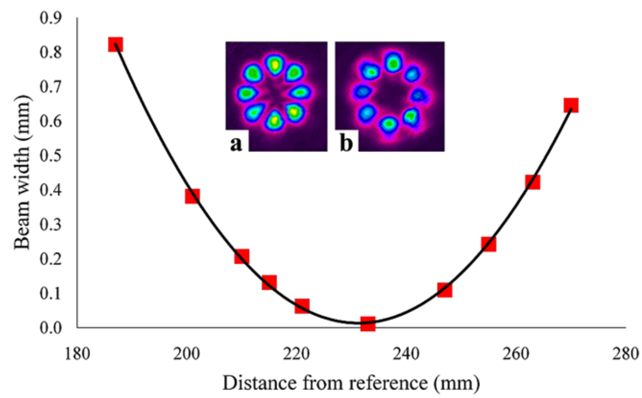

Fig. 6 Measurement of the beam width upon propagation through a lens in the determination of the beam quality factor. The data points are fitted with a second order polynomial whereby the coefficients are used to determine the waist width, waist position and the beam quality factor. The *insets* (**a**) and (**b**) correspond to the near-field and far-field beam intensities, respectively, which indicates that these modes are eigenmodes of the cavity

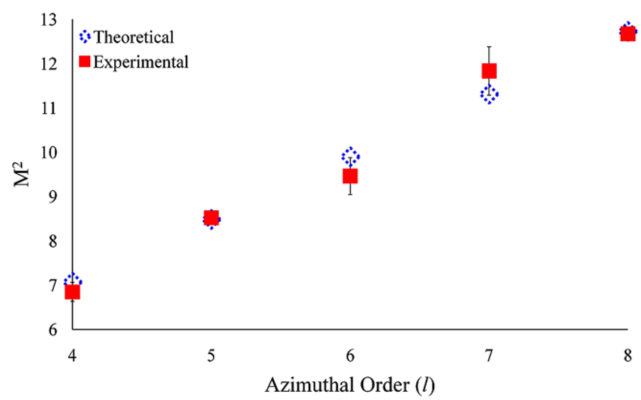

Fig. 7 Theoretical prediction of the beam quality factor for a superposition of LG modes compares well to experimentally measured values, for all azimuthal orders

The results of Figs. 6 and 7 indicate that the field from the laser is the Fourier transform of itself (near fields and

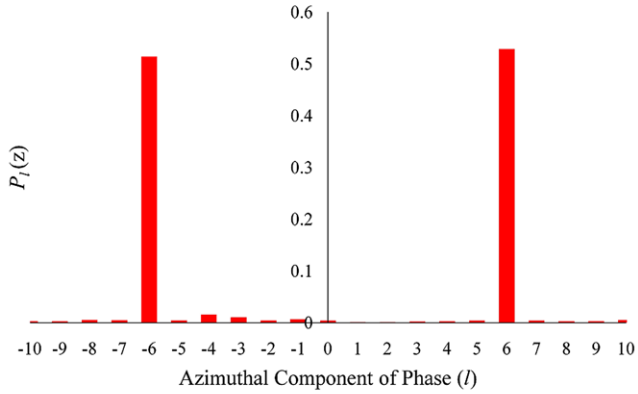

Fig. 8 The relative weighting of the azimuthal components is measured from a modal decomposition of the petal field where the power contained in each azimuthal mode is determined as in (11). The azimuthal component (l) of the match filter in the inner product was varied from -10 to $+10$ and the intensity at the midpoint of the field in Fourier plane of a 12-petal field indicates that this field is superimposed between a $LG_{0,+6}$ and $LG_{0,-6}$ mode

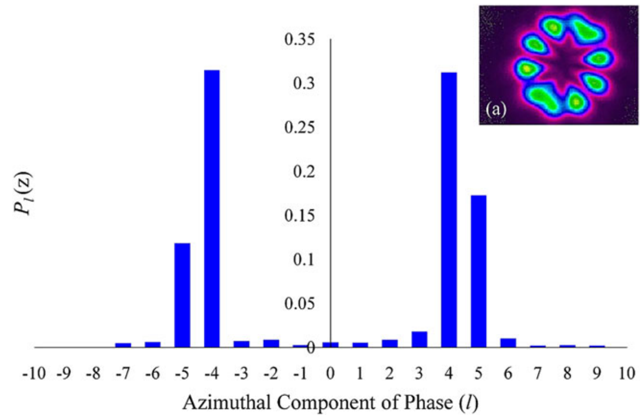

Fig. 9 A modal decomposition analysis for a non-equally weighted superposition of $LG_{0,\pm4}$ and $LG_{0,\pm5}$ modes generated from a misaligned system, where the *inset* (**a**) represents a single frame excerpt (Media 1). The accuracy of the results indicates that this technique of modal decomposition is an extremely robust approach in the analysis of superimposed fields

far field are the same apart from a scale factor), and that the propagation is consistent with that of a coherent superposition of modes, as per our hypothesis.

The modal decomposition of the field was then executed to directly measure the weighting of the azimuthal components. The azimuthal component (l) of the phase pattern on the SLM was varied from -10 to $+10$, and the weighting of the azimuthal harmonics found by an optically executed inner product. Figure 8 shows the results for the 12-petal field (as an example): clearly the field is an equally weighted superposition of harmonics with l of -6 and $+6$, and zero for all other harmonics (within experimental error). In the Laguerre–Gaussian basis, this implies that we have verified our hypothesis. This method of analysis is extremely robust: when the laser cavity was slightly misaligned so as to fall between the conditions for the $LG_{0,\pm4}$ and $LG_{0,\pm5}$ cases, a non-equally weighted superposition of four modes is found, illustrated in Fig. 9 and a mixing of the modes is represented by the inset, Fig. 9(a) (Media 1) which is a single frame excerpt.

Thus we have shown that indeed our cavity is able to produce a coherent superposition of two LG_{0l} modes yielding petal-like intensity patterns as the output. Furthermore, the handedness of the modes can be adjusted: we illustrate in this study from $|l| = 4$ up to 8, but in principle this is limited only by the physical dimensions of the system under study and the amount of gain available. There are then only two issues remaining that warrant some further analysis and discussion: (i) Why does the cavity result in a coherent superposition and not an incoherent superposition? (ii) What is the origin of the confusion in the literature as to what constitutes a pure LG_{0l} mode and what constitutes a superposition of LG_{0l} modes? The latter of which gives rise to a field with $2l$ nodes in the azimuth, resulting in a pattern of "petals" while pure LG_{0l} modes are represented by a circular field with a hollow center.

In the case of the (i), we argue that due to the symmetry of the cavity the resonator cannot distinguish between the left and right handed azimuthal modes, and hence they have equal losses. The very small misalignment of the disk resulting in the oval patterns is a minor perturbing factor, but appears not to be significant enough to distinguish between the handedness of the modes. One can also understand the formation of the superposition from spontaneous symmetry breaking arguments, where the laser modes may have symmetries that are subsets of that of the cavity [24]. We noted in experiments that during propagation of the petal-like field there is no rotation in the intensity pattern in the azimuthal angle and hence the modes have the same phase velocity [25]. The Gouy phase shift is also identical for both modes, and it is easy to show that some arbitrary phase offset in one mode results only in a rotation of the petal pattern by half of this value. Since the flat mirror fixes the waist plane, the consequence of the above is the coherent superposition of the modes. Regarding point (ii), some authors refer to the petal-like structures as pure Laguerre–Gaussian modes [15, 26], and modes as described by (1) as superpositions. Certainly it is true that a superposition of two modes with a relative phase difference of $\pi/2$ will result in an azimuthal dependence of $\cos(l\phi) + i\sin(l\phi) = \exp(il\phi)$ which is of course the same as (1). But this is nothing more than a projection of the phasor in the complex plane onto the real and imaginary axis, and not a new physical construct. The origin of the argument in writing the pure LG_{0l} mode as $\cos(l\phi)$ is because this represents the real part of the electric field, which is the only quantity having a physical meaning. However, the measureable quantity is not the real part of the field squared $(\mathrm{Re}[u])^2$, but uu^*, and further-

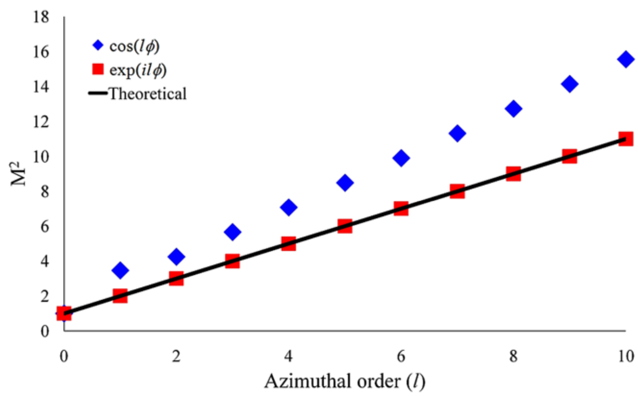

Fig. 10 Beam quality factor determination by a theoretical analysis for a single Laguerre–Gaussian mode of zero radial order where the phase component is chosen as either $\cos(l\phi)$ or $\exp(il\phi)$. LG_{0l} modes which possess $\exp(il\phi)$ match identically the theoretical expression of the beam quality factor ($M^2 = 2p + |l| + 1$) indicating the need for defining LG_{0l} modes as having a phase variation of $\exp(il\phi)$

more $\cos(l\phi)$ does not represent a helical structured wavefront with a Poynting vector tilted relative to the propagation direction, whereas it is known [9] this is the solution to the wave equation for orbital angular momentum carrying fields. Finally one should note that parallels between quantum mechanics and paraxial optics imply that modes of the form $\exp(il\phi)$ always have eigenvalues of $l\hbar$ per photon of OAM in the z direction, and indeed this fact has been the foundation for the use of the LG_{0l} mode as the new basis for describing quantum states. From a purely classical argument, the beam quality factor of the LG_{pl} mode is well known, taking the form of $M^2 = 2p + |l| + 1$, and clearly differs from the value predicted by a $\cos(l\phi)$ phase dependence for zero radial order (see Fig. 10). Note that there is of course a difference between the beam quality factor for a single LG_{0l} mode (Fig. 10) and a superposition of two LG_{0l} modes of opposite handedness (Fig. 7).

The mode structures can also be verified external to the cavity. Using a phase-only SLM we have created single mode and superposition modes of fields with $\exp(il\phi)$ phase variations. In Figs. 11(a) and (b) one sees a pure $\exp(il\phi)$ phase variation imparted to a Gaussian input beam, with the result the usual LG_{0l} mode (in this case for $l = 4$) described by (1). In Figs. 11(c) and (d) we create a superposition of two such OAM carrying fields of opposite handedness, and as expected the output is a set of petal-like structures following the form of (3).

In the abovementioned examples, the input fields were modulated in phase only. To create a field modulated by $\cos(l\phi)$ would require complex amplitude modulation—i.e., a loss of light through variation of the amplitude across the field (since this function varies continuously from $+1$ to -1). For these reasons we prefer to adopt the usual notation of defining the LG_{0l} modes as having a phase variation

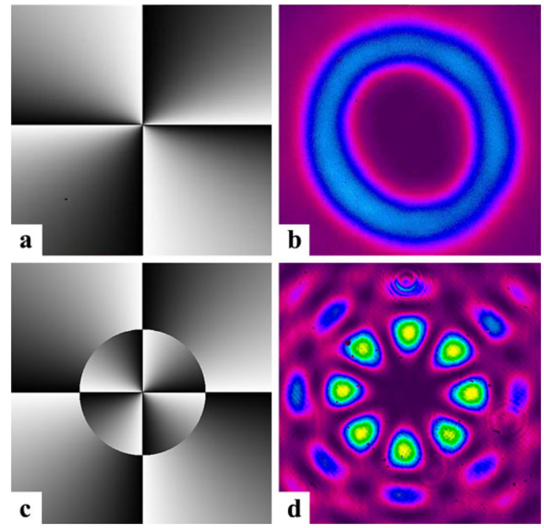

Fig. 11 External to the cavity, generation of single mode or superposition of modes may be achieved with a phase-only SLM. A single LG_{0l} mode is generated by the use of a phase-screen, (**a**), with a pure $\exp(il\phi)$ phase variation where a $LG_{0,4}$ mode, (**b**), is obtained at the output. A superposition of two modes of opposite handedness of order 4 requires a phase screen, (**c**), of two separable azimuthally varying phases which produces a petal structure, (**d**)

of $\exp(il\phi)$, and thus describe our petal-like modes as a superposition of two pure LG_{0l} modes.

5 Conclusion

We have successfully demonstrated a means to generate a coherent superposition of two LG_{0l} modes yielding “petal” modes in a standard Fabry–Pérot laser cavity. The set-up is simple and does not need anything special except a stop, and we have shown that by adjustment of the stop we can produce modes up to azimuthal order 8. Even with the non-ideal method of misaligning a single stop, the comparison between theory and experiment is excellent, and one would anticipate the formation of the petals of higher orders to be ideal if the stop size could be controlled (see for example Fig. 2(a)). We have verified the coherent superposition hypothesis suggested by a variety of experimental tests on both the intensity and phase of the field, and in particular through a full modal decomposition of the field. It is interesting to study such superposition fields because of their relevance in quantum information processing with the OAM states of light.

Acknowledgements We wish to thank Dr. Stef Roux, Dr. Igor Litvin, Mrs. Liesl Burger and Mrs. Angela Dudley for the invaluable discussions and useful advice.

References

1. I.A. Litvin, A. Forbes, Opt. Express **17**, 15891 (2009)

2. I.A. Litvin, A. Forbes, Opt. Lett. **34**, 2991 (2009)
3. P.A. Bélanger, C. Paré, Opt. Lett. **16**, 1057 (1991)
4. C. Paré, P.A. Bélanger, IEEE J. Quantum Electron. **28**, 355 (1992)
5. Y.F. Chen, Y.P. Lan, Appl. Phys. B **73**, 11 (2001)
6. L.Y. Wang, G. Stephan, Appl. Opt. **30**, 1899 (1991)
7. E. Cagniot, M. Fromager, T. Godin, N. Passilly, M. Brunel, K. Aït-Ameur, J. Opt. Soc. Am. A **28**, 489 (2011)
8. D. Naidoo, T. Godin, M. Fromager, E. Cagniot, N. Passilly, A. Forbes, K. Ait-Ameur, Opt. Commun. **284**, 5475 (2011)
9. L. Allen, M.W. Beijersbergen, R.J.C. Spreeuw, J.P. Woerdman, Phys. Rev. A **45**, 8185 (1992)
10. J.A. Rodrigo, A.M. Caravaca-Aguirre, T. Alieva, G. Cristóbal, M.L. Calvo, Opt. Express **19**, 5232 (2011)
11. G. Molina-Terriza, J.P. Torres, L. Torner, Nat. Phys. **3**, 305 (2007)
12. A. Dudley, M. Nock, T. Konrad, F.S. Roux, A. Forbes, Opt. Express **18**, 22789 (2010)
13. S.F. Pereira, M.B. Willemsen, M.P. van Exter, J.P. Woerdman, Appl. Phys. Lett. **73**, 2239 (1998)
14. Q. Deng, H. Deng, D.G. Deppe, Opt. Lett. **22**, 463 (1997)
15. Y.F. Chen, Y.P. Lan, S.C. Wang, Appl. Phys. B **72**, 167 (2001)
16. F.T. Arecchi, Physics D **86**, 297 (1995)
17. S.A. Akhmanov, M.A. Vorontsov, V.Yu. Ivanov, A.V. Larichev, N.I. Zheleznykh, J. Opt. Soc. Am. B **9**, 78 (1992)
18. G. Grynberg, A. Maître, A. Petrossian, Phys. Rev. Lett. **72**, 2379 (1994)
19. A. Ito, Y. Kozawa, S. Sato, J. Opt. Soc. Am. A **27**, 2072 (2010)
20. A. Vaziri, G. Weihs, A. Zeilinger, J. Opt. B, Quantum Semiclass. Opt. **4**, S47 (2002)
21. P.A. Belanger, Opt. Lett. **16**, 196 (1991)
22. A.E. Siegman, IEEE J. Quantum Electron. **27**, 1146 (1991)
23. A.E. Siegman, SPIE Opt. Reson. **1224** (1990)
24. C. Green, G.B. Mindlin, E.J. D'Angelo, H.G. Solari, J.R. Tredicce, Phys. Rev. Lett. **65**, 3124 (1990)
25. R. Vasilyeu, A. Dudley, N. Khilo, A. Forbes, Opt. Express **17**, 23389 (2009)
26. Y.F. Chen, Y.P. Lan, Phys. Rev. Lett. **63**, 063807 (2001)